

Enhanced Nonlinear Pulse Compression from Supercontinuum Generation within Sign-Alternating Dispersion Waveguides

Haider Zia^{1*}

¹ University of Twente, Department Science & Technology, Laser Physics and Nonlinear Optics Group, MESA+ Research Institute for Nanotechnology, Enschede 7500 AE, The Netherlands

**h.zia@utwente.nl*

Abstract

Supercontinuum generation (SCG) coherently generates a wide spectrum from a narrow bandwidth optical pulse. We have recently demonstrated a large increase in the bandwidth to input peak power efficiency of the SCG process, by repeatedly alternating the sign of dispersion along a waveguide. Here, novel properties of SCG in these waveguides are explored. Such as their applicability in SCG resonators and a near parabolic SCG spectral phase independent of higher order dispersion along the alternating waveguide. In order to explain this phase independence a previously unknown normal dispersion SCG phase effect is described. The resultant low higher order spectral phase coefficients, combined with the enhanced bandwidth at low input peak powers, than makes alternating dispersion waveguides a scheme that demonstrates potential to extend sub-cycle pulse compression to low input peak powers, removing the need for high powered drive lasers. In addition, a new scheme is shown for the design of practical waveguide segments that can compress SCG pulses to near transform limited durations which is integral for the design of these alternated waveguides. These results are also applicable to general SCG waveguides and nonlinear pulse compression experiments.

Introduction

Supercontinuum generation (SCG) in Kerr nonlinear waveguides has been exploited in numerous applications such as in the creation of sub-cycle pulses[1-5], metrology using optical frequency combs[6-10], optical coherence tomography[11-13] and as a wide-bandwidth source for ranging and sensing applications[14,15]. However, spectral generation along the propagation of the waveguides ceases due to the interaction of self-phase modulation (SPM) and dispersion, ultimately limiting the achieved broadened bandwidth[1]. We have recently introduced the concept of repeatedly sign-alternating dispersion along the propagation direction as a means of overcoming spectral stagnation that results from this interplay in SCG waveguides (Fig. 1a) [16]. The alternated waveguide structure leads to larger, by potentially several orders of magnitude, input power-to-spectral e^{-1} bandwidth scaling for supercontinuum generation and a flat topped spectral energy density distribution. This is shown in the comparison of our concept with a typical SCG waveguide experiment found in literature [17] (Fig. 1b, 1c).

Here, we consider repeatedly sign-alternating structures where spectral generation occurs primarily in normal dispersion (ND) segments. When spectral generation stagnates due to temporal broadening of the optical pulse, the subsequent anomalous dispersion (AD) segment compresses the pulse to, ideally, its transform limited duration. The temporally compressed pulse then can resume spectral generation in the next ND segment. Limiting SCG to the normal dispersion segments of the alternating waveguide ensures that the SCG has a smooth spectral energy density and phase profile free of modulations.

While our concept opens the possibility to greatly enhance bandwidth generation, many open questions are still unresolved. Firstly, due to the nonlinear generation, the ND and AD segment lengths typically follow a complex arrangement and change along the waveguide. This is inconvenient when periodic arrangements of segment lengths are warranted such as in resonator configurations. Here we report a regime of input pulse parameters where our repeated sign-alternating waveguide has constant ND and AD lengths, independent of input pulse peak power.

Another open question is that the repeated spectral generation and temporal compression of our concept may render that it is sensitive to higher than second order dispersion, practically always present, in the ND and AD segments. For example, this higher order dispersion in the ND and AD segments may introduce a complex spectral phase profile, that impacts temporal compression in the AD segments, limiting the total bandwidth generation. As well, the complex spectral phase that may iteratively build up across the structure would render the concept unfeasible for nonlinear pulse compression experiments. Thus, a solution to this problem would both provide a deeper understanding of what

the AD segment GVD profiles need to be and would make our concept feasible as a method for nonlinear pulse compressions.

To address this problem, we experimentally found [16] that the maximal amount of higher than second order spectral phase contribution (i.e., at the end points of the spectral bandwidth) is *reduced by more than a factor of three* relative to just linear propagation through the waveguide structure. In this paper, we explain this observation by introducing a previously unknown spectral phase effect of normal dispersion SCG. This effect reduces higher order spectral phase coefficients so that the spectral phase remains near parabolic despite significant uncompensated third order dispersion (TOD). This optical SCG effect can be seen as the compliment to the normal dispersion optical wave-breaking effect [18]. Instead, here, the contributions to higher order spectral phase coefficients of higher order dispersion is in turn reduced by SPM. We find that this robustness to higher order dispersion of the bandwidth generating ND segments, is amplified within our alternating waveguides structures. This effect explains more rigorously why, in general, ND SCG has a near parabolic spectral profile, numerically or experimentally found in various experiments in the last decade [19-22].

Within the context of repeated sign-alternating dispersion SCG waveguides this robustness effect combines a near parabolic spectral phase with a large bandwidth for the output SCG pulse. Thus, these waveguides are a lucrative concept in obtaining large nonlinear pulse compression to sub-cycle durations — at low pump powers. As well, the AD segment GVD profiles that maximize pulse compression can be found from this effect. The concept then opens up the possibility of high-quality nonlinear compression for a greater plethora of optical systems such as for high repetition rate lasers and for the integrated photonics setting.

Practically obtaining the needed AD segment GVD profile then becomes the final open question we address in this paper. The AD segment GVD profiles must satisfy strict requirements on its shape if it were to accomplish maximal pulse compression. Moreover, the AD segment GVD profiles change along the repeated sign-alternating structure, since the bandwidth increases of the ND segments decrease along the structure. To address this open ended question, here, we propose a novel scheme to construct arbitrary AD dispersion profiles by breaking up the AD segment into sub-segments that solve a set of linearly independent equations. This procedure can be used for general pulse compression experiments as well.

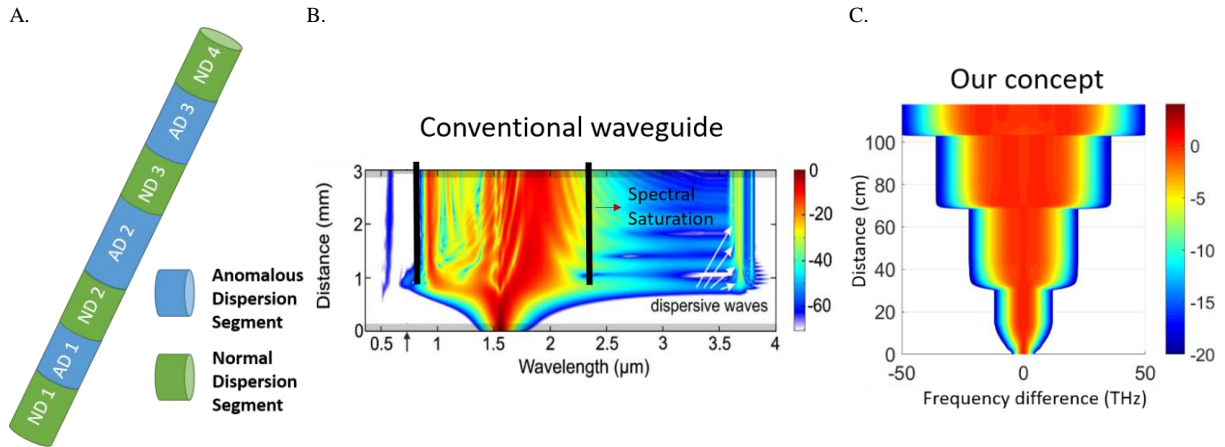


Fig. 1. A) Example schematic of the repeated sign-alternating dispersion waveguide consisting of normal dispersion segments (ND) followed by anomalous dispersion segments (AD). B) Conventional waveguide SCG [17]. Black lines were inserted to highlight the spectral saturation that takes place specifically at the e^{-1} bandwidth (although saturation is visible throughout the entire bandwidth range), past roughly 1 mm of propagation in this particular waveguide. Non-smooth spectral features such as modulations and gaps are clearly visible. C) Plotted is the spectral energy density, in this case, in the spectral generating ND segments of a repeated alternating dispersion waveguide where the AD segments only temporally compress the pulse. The bandwidth increases notably at the $1/e$ do not saturate versus propagation and the spectrum is smooth and continuous.

Periodic Segment Length Convergence

We start by addressing the question of finding ND and AD segment lengths that converge to a fixed arrangement. These segment lengths are set by the amount of spectral broadening that occurs in a segment, and the length until where this spectral broadening saturates, defined as L_{sat} . In general, segment lengths must be chosen for maximum

nonlinear generation and best pulse compression for substantial spectral broadening advantages in such structures. Segment lengths are then heavily influenced by the nonlinear length, $L_{nl} = \frac{1}{\gamma P}$, γ being the waveguide kerr coefficient carrying units of $\frac{w}{m}$, P being the input peak power, and the dispersion length, $L_D = \frac{\tau_o^2}{|d_2|}$, τ_o is the intensity e^{-1} half duration of the pulse entering a segment, d_2 is the group velocity dispersion coefficient [18].

The relative magnitude of these characteristic lengths to each other dictate what regime of supercontinuum generation the pulse is undergoing at a segment in the alternating dispersion structure. For $R \equiv \frac{L_{nl}}{L_D} < 1$, the regime is dominated by nonlinear generation through self-phase modulation (SPM), while for $R > 1$ the regime is dispersion dominated.

In the SPM dominated regime, the spectral bandwidth enhancement due to nonlinear generation occurs primarily within the nonlinear length of the segment. Past this length, the added bandwidth accelerates the dispersive spreading of the pulse, such that final spectral saturation takes place in a distance less than the original dispersion length of the pulse entering the segment.

The dispersion dominated regime is when the additional bandwidth increase from the nonlinear generation is much less than the original bandwidth. Here, the pulse temporally spreads in approximately the same way as the original pulse would spread. The dispersion dominated regime sees much less spectral generation than the SPM dominated regime.

Moreover, R decreases for higher segment numbers in the waveguide, due to the additional frequency generation across prior segments [16], yielding shorter transform limited pulse durations. Thus, at the end of the waveguide, the region would have likely transitioned to the dispersion dominated regime, even if it was SPM dominated at the start of the waveguide structure. In sum, the decreasing R ratio has the effect of uniformly decreasing both the saturation length and the amount of spectral broadening. For a fixed ND segment length, this translates to a decreasing AD segment length, however, we show that this length converges to a fixed constant length above zero. We show this by obtaining an expression for the AD segment lengths in the heavily dispersion dominated regime ($R \gg 1$).

In the dispersion dominated limiting case, simple expressions can be obtained, since the spectral bandwidth increase at the e^{-1} per segment is then given by[16]:

$$\delta\nu \approx \left[g_o \gamma_2 \frac{E}{4|\beta_2|} \right], \quad \text{Eq. 1}$$

with $g_o \approx 0.81$ being a constant related to the Gaussian pulse shape, and with E being the pulse energy.

The corresponding saturation length in the ND segment for this regime would be $L_{sat} = 2L_D$. From this the AD segment length equates to, $L_{AD} \approx (L_{ND} - L_{sat}) \left(\frac{d_{2,ND}}{d_{2,AD}} \right) + 2L_{D,AD} (1 - \delta\nu\tau_o)$. Since $\delta\nu$ stays constant while the initial pulse duration entering the ND segment decreases as segment number increases, the AD segment length converges to $L_{AD} = (L_{ND}) \left(\frac{d_{2,ND}}{d_{2,AD}} \right)$.

This has an importance consequence: Namely, for a constant ND segment length, the AD segments converge to a constant length as well, when the dispersion dominated regime is obtained. Then, periodic waveguides can be constructed, where the spectrum will always increase by Eq. 1, provided losses are negligible.

The dynamics within this regime provides another option for the sign-alternating segmented dispersion waveguides: Instead of maximal spectral increase within a few segments, where segment lengths become complicated, one can use a simple periodic arrangement of highly dispersive segments to achieve the same spectral bandwidth, albeit with many more segments.

When the supercontinuum generation is SPM dominated, or in a transition region in between, ($R \approx 1$) full numerical simulation would have to be carried out to obtain AD segment lengths.

Effects of Uncompensated Spectral Phase and Losses

Eventually, losses and uncompensated spectral phase terminate the enhanced spectral generation of the sign-alternating dispersion waveguide structures.

The effect of losses is easily seen in the dispersion dominated regime, where a constant loss factor, $\alpha \leq 1$, between ND segments in the chain would result in a total spectral bandwidth increase of: $\left(\frac{1-\alpha^n}{1-\alpha} \right) \delta\nu$, where n is the number of ND segments of the segmented waveguide. The total spectral bandwidth increase then converges to a constant, $\left(\frac{1}{1-\alpha} \right) \delta\nu$, for large segment numbers instead of a linearly increasing function of segment number in the case where no losses are present.

Within the SPM and dispersion dominated regime, uncompensated spectral phase, ultimately lowers the same parameter as losses, of which nonlinear generation depends on in the ND segment: Namely, the peak intensity of the pulse entering the ND segment. However, it goes further by also increasing the pulse duration which in addition limits the total nonlinear spectral generation in the segment by effectively lowering the interaction length.

Ideal Dispersion profiles of Segments in the SPM Dominated Region

To address the second question outlined in the introduction, we describe a previously unknown effect that shows that a spectral phase profile independent of the ND GVD profile shape emerges as a consequence of SPM in normal dispersion. In the context of our repeated sign-alternating waveguides, this is the driving effect behind the near parabolic phase obtained at the substantially increased bandwidths these waveguides offer. We show in more detail this effect through representative numerical examples.

To start the discussion we consider a flat ND GVD profile. In this case, higher order spectral phase and spectral amplitude modulations from SPM that originate in the wings of input pulses are removed by the well-known optical wavebreaking effect [18]. Thus, the spectral phase would be near-parabolic, and the ideal AD segment GVD would be flat. For all considered ND segments, the GVD coefficient is sufficiently larger than zero such that higher order spectral phase and modulations originating by SPM in the pulse wings are only negligibly present.

However, the potential complexity arises when the ND segment GVD profile is non-flat, e.g., has substantial third order dispersion. To demonstrate this situation we perform a numerical study using the ND segment group velocity dispersion profile of [16], i.e., of a well-known fiber called Hi1060flex. The GVD of this fiber is shown in Fig. 2a, plotted along the envelope angular frequency range of interest -15 THz to 15 THz. The carrier angular frequency is approx. 1213 THz corresponding to a central wavelength of 1.55 μm . We find that the the example numerical case where we input a transform limited Gaussian pulse (intensity e^{-1} of 72 fs), centered at a pulse energy of 2 nJ represents the characteristic spectral phase evolution of the SCG pulse.

We first plot, in Fig. 2b, the e^{-1} angular frequency bandwidth of the spectral energy density, $\Delta\nu$, against the propagation distance, Δz , within the ND fiber. The resulting saturation curve is characteristic of spectral bandwidth development in ND SCG. We show this propagation up to 30 cm; the saturation length of the bandwidth development.

The simulations show that the spectral phase remains near parabolic despite the shape of the GVD profile of the ND segment. This is because the 3rd order spectral phase coefficient, β_3 , decreases when SPM causes the frequency bandwidth to increase more rapidly than spectral phase additions from third order dispersion. These conditions are met within the saturation length of the fiber. Thus, in order to show that SPM renders that the SCG spectral phase remains near parabolic, despite higher order dispersion, it is first necessary to show the reductive effect of SPM on the 3rd order spectral phase coefficient. We take the comparison of the 3rd order spectral phase coefficient with SPM to without SPM along the propagation to show the reductive effect on this coefficient due to SPM despite higher order dispersion (Fig. 2b). The 3rd order spectral phase coefficient without the influence of SPM is given by $d_3\Delta z$, d_3 is the waveguide TOD coefficient, plotted against ND fiber length (Δz).

The behavior of the ratio of 3rd order spectral phase coefficient is dictated by both the decrease in transform limited duration as a function of increasing bandwidth, through the corresponding TOD length and the rate of bandwidth increase. The ratio remains below one throughout the propagation within the waveguide. This is explained by the cubic dependence of this coefficient to bandwidth, so that, even in regions where spectral generation is reduced, a substantial reductive effect is still present. The ratio grows at first, to about 90 percent and then descends to a minimum of 13% at about 20% L_{sat} . In the region where bandwidth saturations starts to take place, the ratio then grows again and eventually approaches 1 slowly, in the asymptotical limit. However, even at the saturation length, the ratio is still only 74%. We present a more rigorous explanation of the variation of this ratio with propagation distance in the supplementary section.

Secondly, it is important to show that the variation of second order spectral phase coefficient with SPM is slowly varying relative to SPM's impact on the 3rd order coefficient. If this condition is met, the 3rd order spectral phase coefficient reduces more rapidly than the 2nd order coefficient; SPM then renders a near parabolic phase profile of the SCG pulse despite higher order dispersion.

As opposed to the 3rd order phase coefficient that depends on $\Delta\nu^3$, the second order phase coefficient depends on $\Delta\nu^2$ (supplementary for more details). Thus, the reductive effect of SPM on this spectral phase coefficient is expected to be much less. As with the 3rd order phase coefficient, we plot the ratio of second order phase coefficient with SPM to the case without, i.e. to $d_2\Delta z$, versus propagation in Fig. 2d. The general trend of this ratio with propagation should be similar to the 3rd order phase coefficient ratio, e.g, there should be an initial peak, then trough with an asymptotic

rise to 1. However, the lower dependence on spectral bandwidth has the effect of stretching out the curve, that the initial peak is much larger than one, and that the trough is shallower, and occurs even past the saturation length. In fact, we find only a 0.4% reduction of the second order coefficient at the saturation length relative to the linear case. Thus, we find here that second order dispersion does not reduce as strongly with SPM.

Since, 3rd order spectral coefficient is reduced more than the 2nd order with the influence of SPM, the ratio of the two coefficients reduce along the propagation of the waveguide, i.e., the spectral phase becomes near parabolic regardless of higher order dispersion with the presence of SPM. The variation of this ratio is shown through the plot of the normalized ratio of 3rd to 2nd order phase coefficients, $\left| \frac{1}{\tau_0} \frac{\beta_3}{\beta_2} \right|$, against segment length (Fig. 2c). The ratio with SPM contributions stays well below the same ratio where no SPM is present (i.e., $\left| \frac{1}{\tau_0} \frac{d_3}{d_2} \right|$). In fact, this ratio dips to more than a factor of a hundred less than the linear case (0.2%), indicating a strong convergence to a parabolic profile at 20% the spectral saturation length. Moreover, the ratio stays below the linear case up to the saturation length. Since, $\frac{\beta_3}{\beta_2} = \frac{d_3}{d_2}$ for the ideal GVD of the AD segment, the substantial lowering of this ratio due to SPM, means that the AD profile GVD must be flat in the SPM dominated regime.

The above results indicate that at 20% the saturation length higher order spectral phase is minimized. Furthermore, the SCG bandwidth is close to a factor of three greater than input bandwidth at this segment length. So then, both factors; near parabolic spectral phase profile and substantial bandwidth development make this the ideal ND segment length for the alternating waveguide.

The reductive effect of SPM on spectral phase coefficients, which counters the impact of group delay dispersion, is even more pronounced at higher orders, since they depend exponentially with the frequency bandwidth (e.g., for 4th order, Δv^4 , etc.). Under these conditions, the ideal AD dispersion profile would be a flat profile over the frequency range of interest, no matter the dispersion profile of the ND segments.

We conclude this section by noting that while a flat AD GVD profile is ideal in the SPM dominated regime, this may not be a hard criterion since the waveguide consists of subsequent periods of ND-AD segments. After the pulse emerges from this (non-ideal) AD segment it would still go into a subsequent ND segment, where the nonlinear generation there may reduce the initial higher order spectral phase variation it has. For example, the experimental result of [16] showing that the maximum 3rd order phase contribution, occurring at the endpoints of the 1/e bandwidth of the SCG pulse, is a factor of three less than the linear case is explained by this behavior.

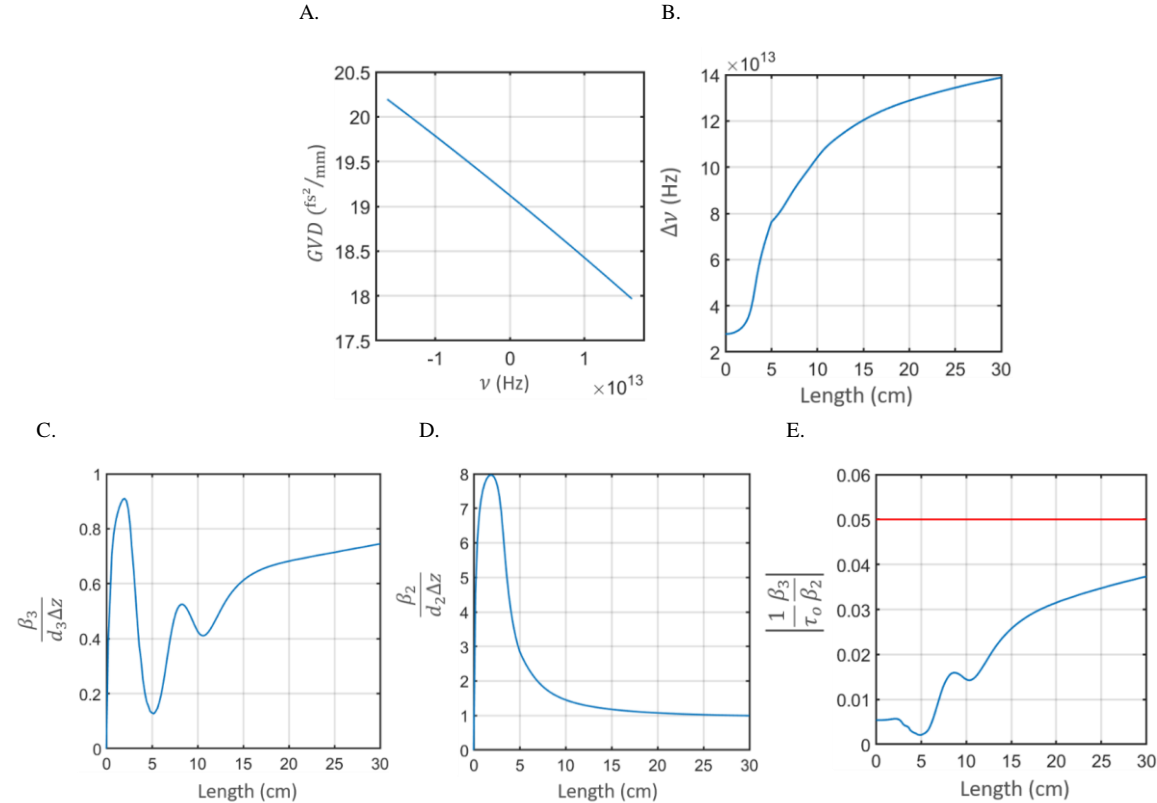


Fig. 2: A) Group velocity dispersion in f_s^2/mm plotted with respect to envelope frequencies, across the bandwidth range of interest in an example normal dispersion fiber. This commercially available fiber, named hi1060flex, was used in [16] to build up the repeated sign-alternating SCG waveguide. B) The e^{-1} angular frequency bandwidth of the spectral energy density (in Hz) versus propagation distance up to the saturation length in the normal dispersion fiber of A). C) Plot of the ratio of the third order spectral phase coefficient, β_3 , of the SCG pulse to the third order spectral phase coefficient in the absence of any nonlinear effect ($d_3\Delta z$) versus the propagation in the normal dispersion fiber of A). D) Plot of the ratio of the second order spectral phase coefficient, β_2 , of the SCG pulse to that when there is no nonlinear effect, ($d_2\Delta z$), versus propagation in the normal dispersion fiber of A). E) Plot of the normalized ratio, $\left|\frac{1}{\tau_0} \frac{\beta_3}{\beta_2}\right|$ indicating the relative magnitude of third order dispersion coefficient to second order dispersion coefficient.

Additional Higher Order Phase Reduction Across Alternating Waveguides

We briefly describe two other phase compensation effects that come into play in the sign-alternating dispersion waveguides. The first is that, the non-flat GVD of Fig. 2a, within an ND segment, results in an asymmetric temporal intensity profile which slows spectral generation on the blue side of frequencies, and enhanced generation on the red side, thus introducing differing saturation lengths for these frequency ranges. Thus, the blue end of the spectral bandwidth is generated at a larger propagation distance in the ND segment compared to the red end. The resultant increase in effective propagation distance for red frequencies and the corresponding decrease for blue frequencies results in a balancing of spectral phase that also reduces higher order contributions. In fact, the sign of β_3 could be reversed due to this phase balancing. This effect also contributes to the near-parabolic spectral phase output of the ND segments regardless of the GVD profile. The sign-reversal may open more possibilities for AD segment choices, that do not need to have opposite sign TOD to the ND segment.

The second is that in the SPM dominated regime of the alternating waveguide structure, the spectral phase becomes closer to parabolic as the pulse traverses the structure compared to the case of a uniform normal dispersion waveguide for SCG. The benefit of the alternating waveguide structure is that the pulse duration inputted to subsequent ND segments decreases, enhancing the higher order spectral phase coefficient reduction. The resultant enhancement is due to the cubic dependence of third order spectral phase on the decreasing transform limited pulse duration.

The low higher order spectral phase coefficients, unique to our alternating waveguide structure, combined with the enhanced bandwidth at low input peak powers, then makes it an effective and powerful new scheme in nonlinear pulse compression experiments. Demonstrating potential to extend sub-cycle pulse compression to low input peak powers, removing the need for high powered drive lasers.

Designing Practically Feasible AD GVD Profiles for General Spectral Phase Profiles

While the above guides the choice of the AD profiles, to obtain these flat profiles is rather difficult. Moreover, there is a transition region from SPM dominated to dispersion dominated for the ND segments in the repeated sign-alternating dispersion waveguide. For these middle ND segments in the chain the ideal AD profiles become unclear. For the dispersion dominated regime, again an entirely different AD segment GVD is sought. Here, the GVD would converge to a scaled reflection of the ND GVD about the frequency axis, with the scaling determining its length.

Even in the SPM dominated regime, due to practical considerations, ND segments may have to exceed their saturation lengths. It is then needed to derive a practical and general method for obtaining both an overall flat AD GVD or any other needed AD GVD such that the pulse obtains a transform limited duration at the end of the segment

We proceed by splitting the AD segment into a number of sub-segments, for the goal of compensating the spectral phase of the pulse coming out of the ND segment. The number of such sub-segments determines the order precision of spectral phase compensation. For example, two sub-segments would compensate up to 3rd order spectral phase, three would compensate up to 4th order and so forth.

Next, for an optical pulse having traversed these sub-segments, perfect spectral phase compensation up to order “n” would be achieved if the segments satisfy:

$$\begin{aligned}
 -\sum_{k=1}^n \beta_{2,k} L_k &= \left. \frac{d^2 \varphi}{d\omega^2} \right|_{\omega_0} \\
 -\sum_{k=1}^n \beta_{3,k} L_k &= \left. \frac{d^3 \varphi}{d\omega^3} \right|_{\omega_0} \\
 &\vdots \\
 -\sum_{k=1}^n \beta_{n,k} L_k &= \left. \frac{d^n \varphi}{d\omega^n} \right|_{\omega_0}
 \end{aligned} \tag{Eq. 2}$$

Where, $\beta_{n,k}$ is the n^{th} derivative of the frequency dependent wavenumber of material indexed by the number k . φ is the spectral phase of the output pulse from the ND segment before these sub-segments. ω is the angular frequency and ω_o is the central angular frequency of the pulse, about where the Taylor series expansion of the spectral phase, describing the entire spectral phase function occurs. L_k is the length of the specific sub-segment.

Eq. 2 can be conveniently represented in matrix form,

$$\mathbf{Ax} = \mathbf{y} \quad , \quad \text{Eq. 3}$$

Where, \mathbf{A} is a $n - 1$ by k matrix formed with the β 's as elements, i.e., $\beta_{j,k}$ (rows labelled by index j , columns by index k). \mathbf{x} is a column vector of segment lengths, and \mathbf{y} is a column vector of increasing derivative orders, starting from 2^{nd} to n^{th} order of the spectral phase of the pulse exiting the ND segment at ω_o .

In general, $\beta_{n,k}$ need not be the same sign, however, materials must be chosen such that at the end all L_k that solve this system of equations must be positive, so that the solution is physically relevant. Also, the materials must be chosen such that n linearly independent equations are guaranteed so that this system of equations does not become over-determined for the set of sub-segments.

In theory splitting the AD segments into a series of sub-segments for pulse compression can compensate for a general spectral phase variation of a pulse entering this system. However, in a practical setting the number of sub-segments is strongly limited by coupling losses in-between these sub-segments.

This puts the strict criteria on the mode field diameters (MFD) of these waveguide segments. It must be roughly the same or must exhibit an adiabatic variation across these sub-segments to minimize losses. Thus, the sub-segments must vary their geometry (e.g., core diameter) in an adiabatic way, or in a perturbative sense in relation to neighboring sub-segments.

This perturbative variation in turn only introduces small changes in the corresponding waveguide $\beta_{n,k}$. Nonetheless, the magnitude of variation of the $\beta_{n,k}$ between two different waveguides (i.e., between two different k indices) does not necessarily impede on the linear independence of the system of equations (Eq. 3). Consequently, the method is compatible for small waveguide variations between the sub-segments.

Instead, small variations in the $\beta_{n,k}$ between two different sub-segments makes that the corresponding length difference between the segments would generally be larger, ultimately introducing longer segment lengths in the sign-alternating dispersion waveguide. In general, this is only a problem if propagation losses are substantial, especially compared to coupling losses that would be introduced if the adiabatic variation between sub-segments is broken.

Conclusions

We explored the conditions that lead to the AD and ND segment lengths of repeated sign-alternating dispersion SCG waveguides to converge to a constant for both segment types. This has ramifications both in the practical design of these structures and whether they can be used in resonator configurations.

Next, we explored the spectral phase development of the SCG where we find an entirely unknown phase effect in supercontinuum generation within normal dispersion waveguides. Namely, that the spectral phase demonstrates robustness to higher order dispersion. This result is amplified within our sign-alternating structures, rendering that our waveguide concept combines a near parabolic spectral phase profile with a substantially increased bandwidth generation. Thus, we foresee that our scheme has potential for sub-cycle pulse compression without the onus of high peak power drive lasers. This then provides an efficient scheme for nonlinear pulse compression for a greater plethora of optical platforms such as for high repetition rate lasers and integrated photonic applications.

We then outlined a practical design method to obtain ideal AD segment GVD profiles needed to compensate all spectral phase terms coming from the corresponding ND segments. These results are not only applicable to repeated sign-alternating SCG waveguides but for general nonlinear pulse compression schemes.

References

1. Dudley, J. M., Genty, G. & Coen, S. Supercontinuum generation in photonic crystal fiber. *Rev. Mod. Phys.* **78**, 1135–1184 (2006).

2. Manzoni, C. *et al.* Coherent pulse synthesis: Towards sub-cycle optical waveforms. *Laser Photonics Rev.* **9**, 129–171 (2015).
3. Hassan, M. T. *et al.* Optical attosecond pulses and tracking the nonlinear response of bound electrons. *Nature* **530**, 66–70 (2016).
4. Hemmer, M., Baudisch, M., Thai, A., Couairon, A. & Biegert, J. Self-compression to sub-3-cycle duration of mid-infrared optical pulses in dielectrics. *Opt. Express* **21**, 28095 (2013).
5. Chen, Hung-Wen, *et al.* "3 GHz, Yb-fiber laser-based, few-cycle ultrafast source at the Ti: sapphire laser wavelength." *Opt. Lett.* **38**, 4927-4930(2013).
6. Yu, M. *et al.* Silicon-chip-based mid-infrared dual-comb spectroscopy. *Nat. Commun.* **9**, 6–11 (2018).
7. Luke, K., Okawachi, Y., Lamont, M. R. E., Gaeta, A. L. & Lipson, M. Broadband mid-infrared frequency comb generation in a Si₃N₄ microresonator. *Opt. Lett.* **40**, 4823 (2015).
8. Schliesser, A., Picqué, N. & Hänsch, T. W. Mid-infrared frequency combs. *Nat. Photonics* **6**, 440–449 (2012).
9. Rieker, G. B. *et al.* Frequency-comb-based remote sensing of greenhouse gases over kilometer air paths. *Optica* **1**, 290 (2014).
10. Holzwarth, R. Optical frequency metrology nature review. **416**, 1–5 (2002).
11. Humbert, G. *et al.* Supercontinuum generation system for optical coherence tomography based on tapered photonic crystal fibre. *Opt. Express* **14**, 1596 (2006).
12. Unterhuber, A. *et al.* Advances in broad bandwidth light sources for ultrahigh resolution optical coherence tomography. *Phys. Med. Biol.* **49**, 1235–1246 (2004).
13. Israelsen, N. M. *et al.* Real-time high-resolution mid-infrared optical coherence tomography. *Light Sci. Appl.* **8**, (2019).
14. Luke, K., Okawachi, Y., Lamont, M. R. E., Gaeta, A. L. & Lipson, M. Broadband mid-infrared frequency comb generation in a Si₃N₄ microresonator. *Opt. Lett.* **40**, 4823 (2015).
15. Schliesser, A., Picqué, N. & Hänsch, T. W. Mid-infrared frequency combs. *Nat. Photonics* **6**, 440–449 (2012).
16. Zia, H., Lüpken, N. M., Hellwig, T., Fallnich, C., & Boller, K. J.. Supercontinuum generation in media with sign-alternated dispersion. arXiv preprint arXiv:1905.01820 (2019).
17. Xie, Shangran, *et al.* As₂S₃-silica double-nanospike waveguide for mid-infrared supercontinuum generation. *Opt. Lett.* **39** 5216-5219(2014).
18. Alfano, R. R. *The supercontinuum laser source: the ultimate white light.* (Springer US, 2016).
19. Heidt, Alexander M., *et al.* High quality sub-two cycle pulses from compression of supercontinuum generated in all-normal dispersion photonic crystal fiber. *Opt. Express* **19**, 13873 (2011).
20. Demmler, Stefan, *et al.* Generation of high quality, 1.3 cycle pulses by active phase control of an octave spanning supercontinuum. *Opt. Express* **19**, 20151 (2011).
21. Sukhoivanov, Igor A., *et al.* Supercontinuum generation at 800 nm in all-normal dispersion photonic crystal fiber. *Opt. Express* **22**, 30234 (2014).
22. Xing, S., Kharitonov, S., Hu, J., & Brès, C. S.. Linearly chirped mid-infrared supercontinuum in all-normal-dispersion chalcogenide photonic crystal fibers. *Opt. Express* **26**, 19627 (2018).